

HALO: A Fine-Grained Resource Sharing Quantum Operating System

John Zhuoyang Ye

University of California, Los Angeles

Jiyuan Wang

Tulane University

Yifan Qiao

University of California, Berkeley

Jens Palsberg

University of California, Los Angeles

Abstract

As quantum computing enters the cloud era, thousands of users must share access to a small number of quantum processors. Users need to wait minutes to days to start their jobs, which only takes a few seconds for execution. Current quantum cloud platforms employ a *fair-share* scheduler, as there is no way to multiplex a quantum computer among multiple programs at the same time, leaving many qubits idle and significantly under-utilizing the hardware. This imbalance between high user demand and scarce quantum resources has become a key barrier to scalable and cost-effective quantum computing.

We present HALO, the first quantum operating system design that supports fine-grained resource-sharing. HALO introduces two complementary mechanisms. First, a hardware-aware qubit-sharing algorithm that places shared helper qubits on regions of the quantum computer that minimize routing overhead and avoid cross-talk noise between different users' processes. Second, a shot-adaptive scheduler that allocates execution windows according to each job's sampling requirements, improving throughput and reducing latency. Together, these mechanisms transform the way quantum hardware is scheduled and achieve more fine-grained parallelism.

We evaluate HALO on the IBM Torino quantum computer on helper qubit intense benchmarks. Compared to state-of-the-art systems such as HyperQ, HALO improves overall hardware utilization by up to $2.44\times$, increasing throughput by $4.44\times$, and maintains fidelity loss within 33%, demonstrating the practicality of resource-sharing in quantum computing.

1 Introduction

Quantum computing has emerged as one of the most promising paradigms for solving problems that are intractable on classical machines, offering exponential speed-ups in applications such as cryptography, optimization, and materials simulation [9, 22, 25, 42]. Over the past decade, rapid advances in superconducting and trapped-ion hardwares have led to the

deployment of cloud-accessible quantum computers by major vendors such as IBM [6, 45], Google [5, 9], and Rigetti [35, 50].

Despite this progress, the quantum computing ecosystem faces a critical hardware bottleneck. The number of available quantum devices is still extremely small, while the global user base continues to grow rapidly. On public platforms such as IBM Quantum, thousands of users share access to a handful of machines, often leading to queues with hundreds or thousands of pending jobs [3]. This mismatch between high user demand and limited hardware capacity poses a serious barrier to scalable and cost-effective quantum computing.

Existing cloud platforms primarily adopt an exclusive-use model, where each submitted job monopolizes the entire quantum device—even if it requires only a small fraction of the available qubits or execution time [1, 2, 4]. As a result, qubit utilization remains low, queue times are long, and the overall throughput of the system is severely constrained. A typical IBMQ cloud service has a queue with up to thousands of pending jobs, and users have to wait for hours to get their results back [3, 47].

To alleviate this bottleneck, we argue that the quantum computing ecosystem urgently needs a *system-level framework* for efficient and flexible resource utilization. Recent efforts toward this goal, such as quantum operating systems (QOS) [19] and quantum virtual machine (QVM) frameworks [47], represent promising first steps. QOS focuses on providing abstractions for program lifecycle management, job submission, and hardware access control, while QVM systems aim to virtualize quantum devices to support concurrent program execution and improve user-level responsiveness. However, despite these advances, existing solutions remain limited in the following two ways.

Limitation 1: Unaware of helper qubit sharing opportunities. Many quantum algorithms rely on *helper qubits* (also known as *ancilla* qubits) that are borrowed temporarily during computation and released afterward [7, 11]. However, existing systems either time-share the entire quantum computer and dedicate all qubits to a single program at a time (e.g., QOS), or statically partition qubits across concurrent programs. They

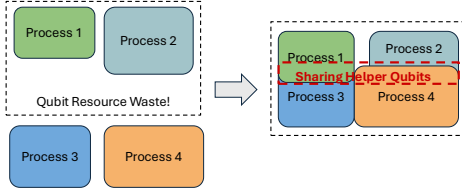


Figure 1: Sharing helper qubits can in principle increase system throughput for applications need a lot of helper qubits.

do not exploit the opportunity to reuse these qubits across concurrent processes, as illustrated in Figure 1.

Limitation 2: Shot-unaware scheduling. Current schedulers in previous work such as HyperQ [47] and QOS [19] assume that all processes need same amount of *shots* (repeated circuit executions for statistical accuracy). However, real quantum applications vary in shot demand. Some fault-tolerant algorithm, such as Shor and Grover’s algorithm, needs only a few shots [22, 42]. Some other recent NISQ algorithms, such as QAOA and random circuit sampling algorithm, need thousands or even millions of shots [9, 25]. As a result, a scheduler that ignores differences in shot requirements cannot properly handle users’ applications in general and fully optimize space-time utilization.

While space sharing and time sharing offer substantial opportunities for improving device utilization, enabling these capabilities in practice introduces several technical challenges.

Challenge 1: Qubit sharing amplifies noise. Sharing helper qubits across concurrently executing processes imposes strict requirements on how each program’s data qubits are mapped onto the hardware [17]. To safely co-locate multiple circuits, the system must place their data qubits sufficiently close to shared helper qubits to avoid excessive SWAP insertion while also ensuring they remain adequately separated to limit crosstalk and unintended entanglement [51]. These constraints couple the mapping decisions of all participating processes, turning what is typically a single-circuit optimization into a joint placement problem with larger search space.

Challenge 2: Shot-aware scheduling requires coordinated temporal multiplexing. The system must evaluate combinations of jobs whose execution windows overlap in time, respect hardware-level concurrency constraints, and avoid unfair allocation patterns. Moreover, scheduling decisions must account for different shot demands so that long-shot jobs do not monopolize the hardware and short-shot jobs do not incur unnecessary waiting.

We develop HALO to address these two challenges and to advance the state of quantum resource scheduling beyond existing approaches summarized in Table 1. IBM Quantum can schedule user processes with different shots but is unaware of helper qubits and doesn’t support space multiplexing. Both QOS and HyperQ support space multiplexing but cannot schedule processes with different shots and is unaware

Feature	IBM [1]	QVM [47]	QOS [19]	HALO
Shots aware	✓	✗	✗	✓(\$3.4)
Space multiplexing	✗	✓	✓	✓(\$3.5)
Helper qubit sharing	✗	✗	✗	✓(\$3.6)

Table 1: Feature comparison among current quantum systems with schedulers. HALO support all features by methods in this paper.

of helper qubit sharing opportunities.

HALO is the first quantum OS design which combine all three scheduling features. More specifically, HALO solves the challenge by using a fine-grained resource sharing mechanism which enables both dynamic space sharing (qubit-level concurrency) and time sharing (shot-aware execution) on real quantum hardware. On the spatial side, HALO supports users to dynamically share the helper qubits between different processes, and minimize the noise with a cost function to jointly optimize qubit placement, routing cost, and noise isolation when multiple programs co-execute on the same device. On the temporal side, HALO incorporates a shot-adaptive scheduler that allocates execution windows according to each job’s shots count and circuit depth. Together, these mechanisms allow HALO to substantially increase quantum hardware utilization while maintaining correctness. We evaluate HALO on three helper qubit intensive benchmarks: the stabilizer measurement circuits, classical arithmetic circuits, and the multi-qubit controlled gates. The main contributions of our paper:

- We design HALO, the first fine-grained resource sharing design that enables multiple quantum processes to safely co-execute on the same quantum device through coordinated space sharing (sharing helper qubits) and time sharing (shot-aware scheduling).
- We develop a hardware-aware multi-process mapping model, including a cost function that accounts for the placement of data-qubit and helper-qubit zone, as well as cross-talk isolation. Our cost functions can explain the fidelity degradation when throughput increase from experiments(§4.6). In addition, we design a shot-aware scheduler that balances processes with different shot requirements to reduce the idle time and improve the batch utilization(§3.4).
- HALO outperforms the state-of-art work by $2.44\times$ on utilization, $4.44\times$ on throughput, while only sacrifice a moderate fidelity loss within 33%(§4.3).

2 Background

Quantum Computing. Quantum computing has emerged as a promising computational paradigm capable of solving

certain problems exponentially faster than classical computers [15, 42]. These capabilities stem from inherently quantum phenomena such as entanglement, which allow quantum programs to explore large computational spaces more efficiently than classical algorithms [26]. As quantum hardware continues to improve, cloud-accessible quantum processors have become increasingly available, allowing researchers across academia and industry to execute real quantum programs [6]. However, the limited number of devices and their constrained qubit resources create significant challenges for scaling quantum workloads, motivating new system-level approaches for efficient resource management [3].

Data Qubits and Helper Qubits. In quantum computation, there are two types of qubits: data qubits, and helper qubits (ancilla qubits) [7, 11, 27, 37]. Data qubits are qubits that store and manipulate key quantum information. Helper qubits, on the other hand, serve an auxiliary role and only have a rather short lifetime. Helper qubits are essential for almost all quantum algorithms at scale. For example, they are used to help make the compilation reversible or more efficient [7, 11, 28, 37]. In fault-tolerant quantum computation, fresh helper qubits are prepared and used to detect error syndromes [41]. Also, lots of helper qubits are necessary in fault-tolerant protocols such as magic state distillation and lattice surgery [10, 31]. One thing is common for helper qubits in all quantum computation: after their jobs complete, they are unentangled with data qubits and can be seen as garbage. Thus, we are able to reuse helper qubits in future computation or even in other processes [17, 28]. Given the common reusability nature of helper qubits, we argue in this research that helper qubits should be seen as a unique type of resources and be managed by the operating system kernel.

Entanglement. Entanglement is a uniquely quantum phenomenon in which the joint state of multiple qubits cannot be expressed as a product of individual states [20, 26]. While entanglement is indispensable for many quantum algorithms, it imposes strict isolation requirements in a multi-tenant quantum system like HALO. Different processes must be unentangled throughout computation. For example, consider two quantum programs P_A and P_B that reuse the same helper qubit q at different points in time. If q is not properly reset after P_A finishes its use, quantum entanglement may cause P_B 's operations to alter the quantum state of P_A , leading to incorrect outputs. Thus, before reassigning a helper qubit, HALO must ensure that it is disentangled and reset to initial state $|0\rangle$. In other words, HALO must carefully control qubit sharing to prevent any cross-process entanglement, ensuring that each job's quantum state evolves independently even while sharing hardware resources.

Quantum process and crosstalk. A quantum program consists of a quantum circuit—a sequence of unitary operations, measurements, and reset instructions—along with a specified number of *shots*, which determines how many times the circuit is repeatedly executed and measured to obtain a classical result [37, 44]. In a multi-tenant quantum system, multiple processes may be mapped onto different regions of the hardware simultaneously [17, 19, 47]. However, physical qubits are not perfectly isolated: superconducting devices exhibit *crosstalk*, where control pulses or two-qubit operations applied to one qubit unintentionally perturb the state or error rates of nearby qubits [51]. Crosstalk can degrade fidelity even when processes do not directly interact, and its effects become more severe when processes are placed too closely or share routing paths. Therefore, HALO must assign qubits and schedule operations in a manner that minimizes interference between processes.

Quantum hardware and layout mapping. There are already many different physical platforms that support quantum computation, such as superconducting [14], trapped ions [12], or neutral atoms [18]. To compile any abstract quantum circuit to all these hardware, finding a good layout mapping from abstract qubit to real qubits is a common problem, due to hardware layout constraints [46], because to connect two remote qubits, we have to add extra noisy routing CNOT gates. In this paper, we consider a superconducting quantum computer with fixed hardware layout graph.

3 Design

3.1 Design Principles

Virtualization of layout, shots and helper qubits. Inspired from the recent seminal work of QVM [47] and QOS [19], we virtualize the space-time resource to facilitate the management and scheduling process [16]. Different from HyperQ, we separate the virtualization of helper qubits and data qubits. In our design, layout of all qubits in the processes are virtualized, and the layout mapping are completely managed by scheduler in QS. Also, we virtualize the shot of each process as an essential time resource.

Fine-grained resource sharing. A central objective of scheduling in HALO is to maximize overall system throughput by increasing the number of programs executed concurrently. To achieve this, the system must maximize the QPU usage qubit-sharing opportunities when many processes want to access the hardware simultaneously. During the space-time scheduling, two quantum processes are expected to share some of the hardware qubits as their helper qubits at different times. Moreover, such opportunities should be exploited as much as possible to maximize the utility of qubit space in

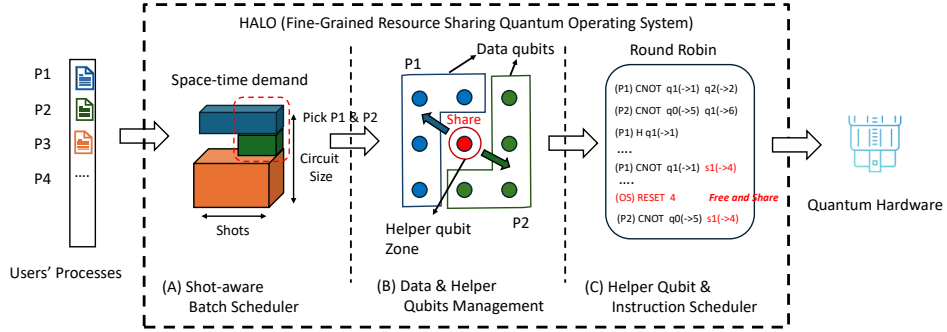


Figure 2: The work flow diagram of HALO scheduler in our resource sharing quantum operating system. It takes user’s processes as input and send scheduled quantum gate instructions to the quantum hardwares.

hardware. Unlike prior systems such as HyperQ [47], which rely on manually specified virtual layouts, HALO performs *automated fine-grained layout synthesis* for concurrently executing circuits. The mapping of all virtual data qubits is a function that accounts for real-device connectivity. At the core of the mapping function is a new cost function that considers multiple constraints unique to multi-tenant quantum execution—routing distance, inter-process crosstalk, and helper-qubit reuse opportunities. This unified objective enables HALO to quantify the safety and benefit of sharing decisions, reducing the extra error caused by noisy routing circuits.

Flexible tradeoff between utilization and fidelity. We provide users with a flexible tradeoff between qubit utilization and fidelity. Through a global system configuration, users can choose to sacrifice fidelity for higher throughput or, conversely, reduce throughput to gain higher fidelity. We believe such flexibility is essential for near-term quantum operating systems, where hardware resources are scarce, and user requirements are highly diverse [3, 19].

Isolation across processes. In the qubit layout mapping across many processes, the scheduler has to make sure that each process is isolated to prevent unintended interference [19, 47]. First, each process’s data qubits are mapped to *disjoint physical regions*, preventing accidental entanglement or crosstalk with other processes. Our placement algorithm explicitly avoids qubit assignments that violate spatial separation constraints by *inter-process crosstalk cost* discussed in Section 3.2. Second, for helper qubits that are shared across processes, HALO enforces a mandatory *reset* operation before reuse, ensuring the qubits are fully disentangled from the previous workload. Together, these mechanisms ensure that each process evolves independently, even while the hardware resources are being multiplexed for improved utilization.

Table 2: System calls for the resource sharing quantum operating system

System Call	Description
<code>q=alloc_data(x)</code>	Allocate x data qubits.
<code>s=alloc_helper(y)</code>	Allocate y helper qubits.
<code>deallocate_data(q)</code>	Release the data-qubit space.
<code>deallocate_helper(si)</code>	Release the helper-qubit s_i .
<code>set_shot(x)</code>	Set number of shots as x .

3.2 Kernel System Call Interfaces

HALO virtualizes data qubits, helper qubits and shots. HALO has five system interfaces provided to processes by the kernel, as listed in table 2. A process should tell the kernel the total number of data qubits and helper qubits, as well as the number of shots it needs. A process asks the kernel to allocate these resources for them by system calls before scheduling starts. A process accesses a virtual data qubit by q_i , and a virtual helper qubit by s_i , where i is the unique index in the one-dimensional virtual space. All classical measurement results are stored in a one-dimensional virtual classical space labeled as c_0, c_1, c_2, \dots . The scheduler sends the instructions to the hardware after allocation.

Unlike HyperQ [47], qubit layouts are completely managed by the space manager in HALO. As a result, programmers are shielded from hardware layout concerns. Thus, our interface design is adaptable to different quantum hardware and layouts, in principle.

3.3 HALO Overview

We introduce HALO, a space-time quantum operating system that performs multi-process management and scheduling as shown in Figure 2. We give an overview of the entire fine-grained scheduling loop. HALO coordinates concurrent execution through a three-stage scheduling pipeline:

1. **Shot-aware batch scheduling (§3.4).** In the first stage, HALO selects a compatible batch of processes from the wait-

ing queue based on space requirements and concurrency potential. After this step, HALO decides to run these quantum processes in the selected batch on the hardware for the same number of shots. 2. **Static data-qubit placement** (§3.5). In this stage, HALO computes an optimized hardware-aware data qubit layout for all processes in the selected batch of the previous step. HALO optimizes a cost function by simulated annealing with some heuristic. All the rest of the unassigned hardware qubits form the helper-qubit zone. 3. **Dynamic helper-qubit routing and instruction scheduling** (§3.6). In the last stage, HALO decides on the final instruction order and dynamic mapping of helper qubits for all batch processes. HALO uses a round robin algorithm for the instruction order, so every process has a fair chance to compete for the public helper qubit zones. HALO greedily assigns the nearest available helper qubits for all instructions. HALO also inserts necessary resets for safe helper qubit reuse, this make sure that all processes are unentangled even if they share helper qubits.

3.4 Shot-aware process batch scheduler

In the first stage, HALO balance the space-time volume of each process batch to improve the throughput of a single QPU. After the space manager determines a layout for each process, each process P has q_p^d data qubits and q_p^h helper qubits. And need to execute s_p shots by calling interface `set_shot(sp)` listed in Table 2. We also denote the circuit depth of the process as d_p .

Let the number of physical qubits on the device as Q_{tot} . HALO introduces a tunable system parameter $0 < \lambda < 1$, the *data-qubit occupancy ratio*, which controls the aggressiveness of spatial sharing. The HALO forms a batch B of processes p_i until the total number of required *data* qubits reaches λQ_{tot} .

Since IBMQ doesn't report the active time for each qubit [47], we estimate the time of a process in terms of its depth of circuit \times shot count. For a process P with q_p^d data qubits, q_p^h helper qubits, circuit depth d_p , and the remaining shot count s_p , the *total depth demand* is $D_p = s_p \cdot d_p$, and the *space-time demand* (work volume) is $W_p = q_p^d \cdot D_p = q_p^d \cdot d_p \cdot s_p$, where Q_p is the number of data qubits it needs. When HALO schedules a batch B of processes that execute the same number of shots s_B , the batch *makespan* is $D_B = s_B \cdot \max_{p \in B} (d_p)$, and the total *space-time capacity* for the batch is $\text{Cap}_B = Q_{\text{tot}} \cdot D_B$. The batch's *useful work* is computed as: $\text{Work}_B = \sum_{p \in B} q_p^d \cdot d_p \cdot s_p$. HALO optimize batch formation using the following heuristic:

1. **Shot and depth aware priority:** Figure 2 shows that resource inefficiency primarily arises from the misalignment between circuit depth and shot count in the process queue. To mitigate this fragmentation, processes are reordered first by jointly considering their shot and depth demands. Specifically, processes with smaller total depth demand $D_p = s_p \cdot d_p$ are assigned higher priority. s_p is the

remaining shot count and will be updated after batch execution. Similar priority heuristics are used in coflow scheduling in classical data-parallel clusters [13].

2. **Qubit capacity constraint:** After reordering the arrived processes in queue by the priority, HALO greedily choose a batch from the process with the highest priority to the process with the lowest priority. The batch must fit on the device, also, the scheduler optimizes the hardware utility by the *data occupancy ratio*. For example, if $\lambda = 0.6$, HALO take a batch only when the sum of all data qubits uses at least 60% of the hardware qubits.

$$\lambda Q_{\text{tot}} \leq \sum_{p \in B} q_p^d < Q_{\text{tot}}.$$

If all processes in the queue need less than λQ_{tot} data qubits, HALO keeps waiting until reach a maximum time bound that we set in the configuration file(10 second).

3. **Batch shot count:** For the selected batch B , HALO executes the minimum number of shots in the batch:

$$s_B = \min(S_{\text{max}}, \min_{p \in B} s_p),$$

where S_{max} is a tunable maximum number of shots per batch. This prevents very deep processes from creating long batches that waste shot resources, and allows deep jobs to be split across multiple batches. After the batch execution, each process's remaining shots is updated by subtracting $s_p \rightarrow s_p - s_B$. If $s_p = 0$, the process finish and is removed from the queue.

Example. Assume that the hardware device has $Q_{\text{tot}} = 24$ and we set $\lambda = 0.6$. There should be at least 15 data qubits to form a batch. Consider four processes waiting in the queue:

- $P_1: q_1^d = 8$ qubits, $d_1 = 100$, $s_1 = 100$
- $P_2: q_2^d = 10$ qubits, $d_2 = 10$, $s_2 = 60$
- $P_3: q_3^d = 12$ qubits, $d_3 = 12$, $s_3 = 60$
- $P_4: q_4^d = 12$ qubits, $d_4 = 80$, $s_4 = 100$

A shot-and-depth unaware scheduler will take P_1, P_2 as the first batch and execute 60 shots. This batch wastes space-time utility as P_1 and P_2 are misaligned in depth. HALO prioritizes P_2, P_3 first, since $D_2 = 10 \cdot 60 = 600, D_3 = 12 \cdot 60 = 720$ is the smallest two in *total depth demand*. The batch shot count is: $s_B = \min(S_{\text{max}}, \{s_2, s_3\}) = 60$. Thus, HALO executes the batch B containing P_2, P_3 for 60 shots and updates process results accordingly.

Optimization objective. Suppose the scheduler forms a sequence of batches B_1, \dots, B_K . For each batch B_k , let $D_{B_k} = s_k \cdot \max_{p \in B_k} d_p$ denote the batch makespan, where s_k is the

number of shots executed in batch B_k . The corresponding space-time capacity is $\text{Cap}_k = Q_{\text{tot}} \cdot D_{B_k}$. The useful work completed in batch B_k is $\text{Work}_k = s_k \times \sum_{p \in B_k} q_p^d d_p$. In general, we want to maximize the overall space-time utilization:

$$\max_{\{B_k, s_k\}} \eta = \frac{\sum_{k=1}^K \text{Work}_k}{\sum_{k=1}^K \text{Cap}_k} \quad (1)$$

We calculate η for the first batch in the previous example. If the first batch is P_2, P_3 , $\text{Work} = 60 \times (10 \times 10 + 12 \times 12) = 14640$, and $\eta = \frac{\text{Work}}{\text{Cap}} = \frac{14640}{24 \times 60 \times 12} = 0.85$. On the other hand if the first batch is P_1, P_2 , $\text{Work} = 60 \times (8 \times 100 + 10 \times 10) = 54000$, and $\eta = \frac{\text{Work}}{\text{Cap}} = \frac{54000}{24 \times 60 \times 100} = 0.375$. HALO improves η by a factor of 2.27.

3.5 Data qubits space manager

Inspired by the quantum virtual machine [47], we further design a general cost function for our space-time scheduling algorithm. Our method has fewer constraints on hardware connections than HyperQ [46], where the hardware must have a strong space periodic structure. Despite the complexity of the problem, we capture three critical aspects that determine the mapping quality, and we formalize these aspects by cost functions.

Our intuitions are as follows. First, data qubits cannot be shared and must stay in isolated territories, otherwise the computation of different processes might be entangled (§2). Also, data qubits of different processes should be as far from each other as possible to avoid cross-talk, thus meeting our design goal: *isolation across processes* (§3.1). Second, the helper qubit zone, which is defined as the rest of the qubits after mapping all data qubits, should be close to the data qubits in all processes that need helper qubits. This is our design goal for *fine-grained resource sharing* (§3.1). Ideally, all processes should get equal and fair access to the public helper qubit zone. Finally, the circuit topology of data qubits should match the layout, which is well studied in quantum circuit layout synthesis [46].

In HALO’s data qubit space manager, we configure the connection graph $G = (V, E)$ of a fixed hardware, where V are hardware qubits and E are hardware-qubit connections.

Assume that the shot aware process batch scheduler (§3.4) decides to execute m processes P_1, P_2, \dots, P_m . Each P_i has $q_{P_i}^d$ data qubits in total and $q_{P_i}^h$ helper qubits. We denote the set of data qubits for process P_i as Q_i^d . The data qubit manager in HALO further calculate a physical layout L for these processes on G . The mapping L balances routing efficiency among data qubits, crosstalk between multiple processes, and routing efficiency between data qubits and helper qubits. HALO iteratively optimizes a cost function that captures the quality of a joint placement across all processes.

Inter-process crosstalk cost. The first component of the cost function captures the level of mutual isolation between pairs of processes. This is defined as the average distance between all pair of data qubits Q_a^d and Q_b^d between two processes P_a and P_b in the mapping. We denote this cost as $\text{Inter}(L, G)$.

Helper qubit routing cost. All the physical qubits that are not used as data qubits form the helper qubit zone H , where $H = V \setminus \bigcup_i \{L[q_i], q_i \in Q_i^d\}$. HALO has a greedy policy for the helper qubit mapping: any process will greedily find the nearest helper qubits when necessary. Thus, we measure the quality of data qubit layout by the extra routing cost between data qubits that need helper qubits with the helper qubit zone H . We call it *helper qubit routing cost*, denoted as $\text{HRCost}(L, G)$.

Intro-process data qubit routing cost. The routing cost among data qubits is measured by the total number of extra number of SWAP gates needed with a fixed layout to connect remote data qubits, this is the same as the layout cost in the previous layout synthesis work [46]. We denote this cost as $\text{Intro}(L, G)$.

Total layout cost: Let $L : Q^d \rightarrow V$ be a layout mapping all virtual data qubits to hardware qubits, and let $H \subseteq V$ be the helper region. For fixed non-negative weights $\alpha, \beta, \gamma \in R_{\geq 0}$, the total layout score is defined as:

$$\text{Cost}(L, G) = \alpha \text{Intro}(L, G) - \beta \text{Inter}(L, G) + \gamma \text{HRCost}(L, G) \quad (2)$$

Our goal is to find a layout L^* that minimizes $\text{Cost}(L, G)$. In this research, we set $\alpha = 0.5, \beta = 0.3, \gamma = 1$.

In general, finding the optimal layout is NP-hard [34]. We implemented a simulated annealing algorithm to iteratively search for a better mapping of data qubits onto a hardware graph. The algorithm begins with a greedy, process-clustered initial placement, then repeatedly proposes local moves, which are either small swaps within a process or moving a data qubit into a nearby helper site [49].

Example. In Figure 3, we show three different suboptimal layout mappings of data qubits for two processes P_1, P_2 during simulated annealing. 1. If HALO maps $\{5, 0, 1\}$ to P_1 and $\{2, 7, 6\}$ to P_2 , then P_1 is *far from helping-zone*. Such a mapping increases the helper qubit mapping cost $\text{HRCost}(L, G)$. If HALO map $\{0, 2, 8\}$ to P_1 and $\{5, 7, 3\}$ to P_2 , then since there are routing path conflicts and the process mapping is not compact, the cross talk will severely affect process fidelity, this can be capture by a rather small inter-process cross talk cost $\text{Inter}(L, G)$. 3. If HALO map $\{0, 1, 5\}$ to P_1 and $\{4, 9, 8\}$ to P_2 , P_2 and P_1 don’t share helper qubits in between, the sharing opportunity is not optimized. HALO determines a much better data qubit layout mapping, where $\{0, 1, 5\}$ is mapped to P_1 and $\{3, 8, 7\}$ is assigned to P_2 . In this layout, P_1 and P_2 can share hardware qubit 2 in between, and the process cross talk is controlled.

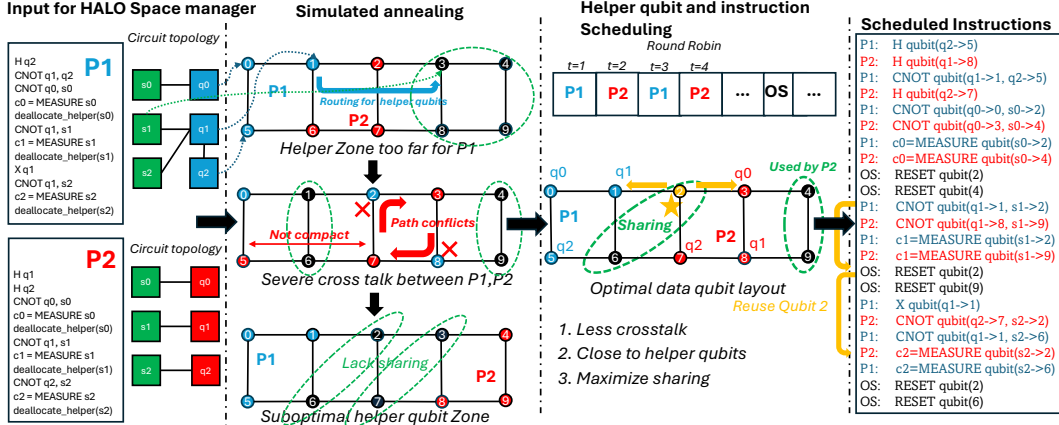


Figure 3: Example of HALO space management and instruction scheduling. HALO schedules a batch of two processes with 12 qubits in total on a 10 qubit quantum hardware (Impossible if not sharing helper qubits). Both P_1 and P_2 have 3 data qubits and 3 helper qubits. We show three suboptimal data qubit layouts, and also the optimal data qubit layout. Right: The full scheduled instructions of the two process batch in a round robin order after HALO fix the data qubit layout mapping.

3.6 Helper qubit and instruction scheduler

This section explains our design of the scheduling of process instruction with helper qubit dynamic mapping. Any virtual helper qubit s_i is dynamically assigned a physical qubit during the instruction scheduling. Let t be the index of the current instruction finished being scheduled. $L^H(t)[s_i] = k$ means the virtual helper qubit s_i at time t is mapped to hardware qubit k .

In HALO, an instruction such as `CNOT q0, s0` is called a *quantum virtual instruction*. The instruction scheduler in HALO replaces every virtual address with a real hardware address. The new translated instruction is called a *quantum hardware instruction*. For example, if $L[q_0] = a, L^H[s_0] = b$, the translated hardware instruction of `CNOT q0, s0` is `CNOT a, b` which is ready to be transpiled and executed.

In this stage, the output of the HALO instruction scheduler is a list of devirtualized *quantum hardware instruction*. A *Round-Robin* style scheduling algorithm is used in HALO to determine the instruction order. All processes have a fair chance to compete for the helper qubit resources when needed [24, 38, 43].

HALO schedules the next instruction for every process in the batch in turn. When process P_a is selected to execute its next instruction I , HALO handles the instruction according to the following logic. If I involves only data qubits, HALO directly translates it via the layout mapping L and appends it to the scheduled instruction list. If I requires helper qubit(s) and sufficient helper qubits are available, HALO greedily selects the nearest available helper qubit, allocates it to I , and schedules the translated instruction. Our design of Helper qubit routing cost in §3.5 is consistent with this step, as the cost function measure how hard for a process to get nearby helper qubits when needed. If I requires helper qubit(s) but none are available, HALO suspends P_a and places it into a waiting state

until helper qubits are released by other processes. Finally, if I is a system call that releases a helper qubit, HALO inserts a hardware reset instruction and marks the corresponding qubit as available for future allocation. The reset instruction make sure that processes are not entangled (§2), and thus the *process isolation* in design principle is satisfied (§3.1).

Example. The right part of Figure 3 shows the full list of de-virtualized scheduled instruction of P_1 and P_2 take turns the run the next instruction. HALO inserts hardware reset instruction when helper qubits are released by system call. In the scheduled instructions, hardware qubit 2 is first assigned to s_1 in P_1 , then reset by HALO, and assigned to s_2 in P_2 . The example reveal the power of sharing helper qubits: P_1 and P_2 have 12 qubits in total if we don't differentiate data qubits and helper qubits, and state of the art quantum space multiplexing system such as HyperQ can put at most one process in execution, with space utility at most 60%.

4 Evaluation

To evaluate the effectiveness of HALO with respect to the challenges (§), we design experiments and answer the following research questions:

- **RQ1(§4.2):** Can we tolerate the scheduling time overhead for a more fine grained hardware control in HALO?
- **Yes,** we measure the scheduling time of HALO of some of the hardest cases in our benchmark suit, and the overhead is below 60 seconds, which is mild compared with hours of waiting time.
- **RQ2(§4.3):** Does HALO perform better compared to state-of-the-art quantum runtime systems?

Yes, we compare HALO against IBM Quantum and HyperQ to quantify improvements over existing cloud execution models. Specifically, HALO achieves $2.4\times$ improvement in space utilization, a $4.44\times$ compared with HyperQ.

- **RQ3(§4.4):** Is sharing helper-qubit really helpful for utilization and throughput?

Yes, we did ablation study by comparing HALO with HALO(No Sharing), which disables helper-qubit reuse to isolate the effect of spatial sharing. We observe that sharing helper qubits increase throughput by a factor $1.52\times$ while increase the fidelity by 11%.

- **RQ4(§4.5):** Is space-time utility η improved by shot-aware scheduling (§3.4)?

Yes, we disable shot-adaptive scheduling to isolate temporal sharing benefits. The shot-aware batch scheduler in HALO consistently improves the space time utility η by a factor of $2.87 \sim 4.04$.

- **RQ5(§4.6):** Does throughput increase affect process fidelity after scheduling?

Yes, we vary the data occupancy ratio λ (§3.4) from 0.2 to 0.8 and observe that the average process fidelity in general decreases while the qubit sharing ratio and throughput increase. The primary contribution is extra noisy routing cost for helper qubits(HMCost in §3.5) when throughput increase.

4.1 Setup

Baselines. We evaluate the performance of HALO scheduling against the following baselines.

IBM Quantum. The current approach used by the IBM Quantum Platform, and other quantum cloud providers, to run each program individually on the entire machine [1, 3].

HyperQ. The quantum virtual machine with fixed layout mapping pattern but not sharing helper qubits [47].

HALO(NoSharing). HALO with shot scheduling and space multiplexing, but with helper-qubit sharing disabled. All qubits are seen as data qubits.

HALO(ShotUnaware). HALO with helper-qubit sharing, but uses shot-unaware scheduling where the process batch a extract in an FIFO order.

Benchmarks. Currently, existing quantum circuit benchmarks such as QASMBench [29], do not distinguish between data qubits and helper qubits. To address this limitation, we introduce a new benchmark suite specifically designed to capture this distinction. Our suite consists of four categories of benchmarks with varying circuit sizes and helper-qubit proportions, which we believe are representative of near-term quantum applications that rely on helper qubits as well as

Suite	#	Name	Data	Helper
I: QEC(Small)	1	shor_stabilizer_XZZX_n3	3	5
	2	syndrome_extraction_surface_n4	4	4
	3	cat_state_verification_n4	4	2
I: QEC(Medium)	4	fivequbit_round_2_error_IIZII	5	16
	5	steane_round_2_error_IIIIIXI	7	12
	6	surface_d3_round_3_error_XIIIIIII	9	24
II: Arithmetic(Small)	7	varnum_3_d_4_1	3	19
	8	varnum_3_d_4_1	4	7
	9	varnum_4_d_4_1	4	8
II: Arithmetic(Medium)	10	varnum_10_d_3_1	10	11
	11	varnum_10_d_4_0	10	19
	12	varnum_12_d_4_1	12	8
III: Multi-CX(Small)	13	mcx_2_0	3	1
	14	mcx_3_0	4	2
	15	mcx_4_1	5	3
III: Multi-CX(Medium)	16	mcx_10_1	11	9
	17	mcx_11_0	12	10
	18	mcx_12_0	13	11
Random	19	data_4_syn_4_gc_15_0	4	4
	20	data_5_syn_5_gc_15_0	5	5
	21	data_6_syn_6_gc_18_0	6	6
	22	data_14_syn_15_gc_45_0	14	15
	23	data_15_syn_12_gc_40_0	15	12
	24	data_20_syn_10_gc_50_0	20	10

Table 3: Some examples in our benchmark suites, which consist of: (I) helper-heavy QEC stabilizer circuits; (II) arithmetic circuits of varying sizes; (III) multi-controlled X circuits; Below are examples of some randomly generated circuits.

the future fault-tolerant quantum computers: (I) Stabilizer measurement circuits(QEC) where all helper qubits served to detect errors [39,41]. We injected a single artificial Pauli error in some programs. (II) Arithmetic circuits. We generate a lot of boolean arithmetic circuits with varying structures and number of variables [23, 48]. (III) A set of Multi-controlled X circuits($C^n(X)$), or quantum condition circuit, which is the most important building block for universal quantum programs and is hard to compile without helper qubits [27,33,53]. Each benchmark has both small scale, and medium scale. (IV) A mix benchmark, which includes all the above with extra randomly generated circuits. Some of the concrete circuit examples are listed in Table 3.

Metric. We evaluate the performance of HALO and baselines based on the following metrics:

Space Utilization Space utilization quantifies how effectively the hardware’s physical qubits are used during execution. It measures the fraction of qubits allocated to active processes(consider both helpers qubit and data qubits) relative to the total number of qubits on the hardware device.

Share Ratio. Share Ratio measures how effectively HALO enables helper-qubit reuse across concurrent processes. It is defined as the fraction of helper qubits that are used by at least two processes during execution. Let H denote the set of all helper qubits, and let $\text{count}(q)$ be the number of processes that use helper qubit q . The Share Ratio is computed as:

$$\text{ShareRatio} = \frac{|\{q \in H \mid \text{count}(q) \geq 2\}|}{|H|}. \quad (3)$$

In helper qubit intense application, a higher Share Ratio indi-

cates that more helper qubits are successfully reused, leading to improved spatial utilization and increased parallelism.

Space-Time Efficiency η . We use the average space-time efficiency η per batch to evaluate the effectiveness of our shot-aware batch scheduling (§3.4). A higher η indicates that the hardware is performing proportionally more useful work rather than remaining idle due to batching inefficiencies.

Process per Batch (PPB). We define *processes per batch* (PPB) as the average number of concurrently executing quantum processes within each scheduled batch. A higher value means larger throughput and lower latency.

Fidelity. We compare the measured output distribution of each circuit against its ideal (noise-free) distribution obtained from a state-vector simulator. We adopt the L_1 distance as our fidelity metric.

$$L_1 = \sum_{s \in \mathcal{S}} |p_{\text{ideal}}(s) - p_{\text{real}}(s)|, \quad (4)$$

where \mathcal{S} is the set of all possible measurement outcomes. The reported fidelity is computed as $1 - \frac{1}{2}L_1$, so that higher values indicate closer agreement with the ideal distribution.

Experimental Setup. To evaluate the performance of the HALO scheduling framework under realistic job submission patterns, we conducted experiments using the standard Poisson distribution as used in HyperQ, where jobs arrive following a Poisson process with a mean rate of 0.6 job per second. We keep generate random job for 40 seconds in all experiments. After scheduling by HALO or other baseline method, we transpiled the circuit and submit through IBM cloud and wait for the result. We did separate experiments to study the space scheduling and the shot-aware time scheduling. In space scheduling experiment, we fix all shots to be the 1000. In the experiment of shot-aware time scheduling, all processes have a randomly generated shots ranges between 500 to 8000.

All experiments were executed on the *IBM Quantum Platform* using the *IBM Torino* quantum processor, which features a *133-qubit square lattice* architecture available for public access. Figure 4 shows a concrete example of HALO manage data qubits of 10 processes on the hardware. Compilation, scheduling, and aggregation of logical jobs into larger composite circuits were performed on a *desktop workstation* equipped with an 12th Gen Intel(R) Core(TM) i5-12400K CPU (2.5 GHz) and 64 GB RAM. All scheduled circuits are further transpiled to the targeted hardware using *qiskit v2.2.3* with optimization level 3.

4.2 RQ1: Scheduling overhead

In experiments, we observe that the running time of shot-aware batch scheduling (§3.4) and instruction scheduling (§3.6) with fixed data qubit layout mapping is negligible (< 0.1 seconds) compared with the space layout optimization (§3.5),

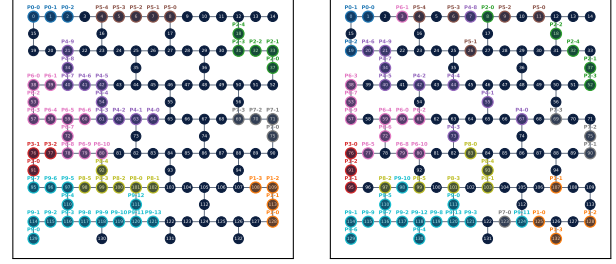


Figure 4: Left: The greedy cluster initial mapping of HALO for a batch with 10 processes on IBM Torino quantum processor. Right: Final mapping decision of HALO after 30 iterations of simulated annealing.

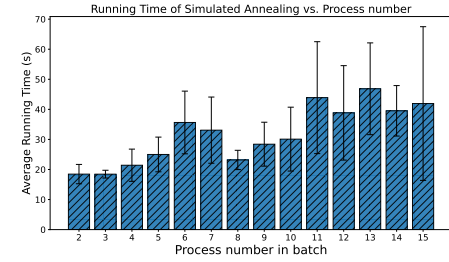


Figure 5: The average running time of HALO’s space management with different number of processes in batch (§3.5). The scheduling ends within 60 seconds for almost all cases, much less than hours of waiting time in current quantum cloud service.

which is the real possible bottleneck. We stress test the total running time of HALO space scheduling of HALO with a fixed number of processes in one batch ranges from 2 to 15. As shown in Figure 5, space scheduling typically completes within one minute, which is negligible relative to the hours of queueing delay on IBM Quantum [3, 47]. Thus, we conclude that HALO’s scheduling overhead is acceptable in the near-term devices with hundreds of qubits.

4.3 RQ2: Overall performance

We compare HALO (fixing the data-occupancy ratio at $\lambda = 0.6$) against IBM Quantum (exclusive-use scheduling) and HyperQ (logical multiplexing without hardware sharing) [47]. As shown in Figure 6 and Table 4, HALO substantially increases the resource utilization and processes per batch relative to both baselines. Compared to the IBM Quantum execution model, which serializes all jobs, HALO increases resource utilization by $5.34 \times$ on average in all benchmarks, while increasing the processes per batch by $10.17 \times$ on average, which effectively saves 90.1% of end-to-end latency for users in a throughput-limited regime. Compared to HyperQ, HALO achieves a $2.99 \times$ improvement in utilization and a $4.44 \times$ increase in processes per batch by jointly removing Hy-

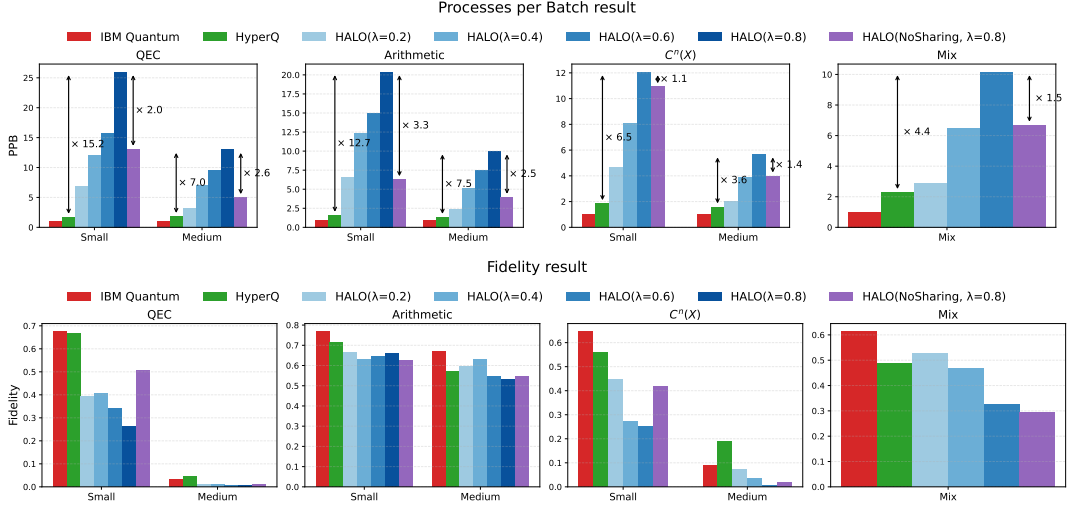


Figure 6: Result of our evaluation. Above: Result of process per batch (PPB) on three benchmarks and the mix benchmark. HALO improve PPB by a factor of $\times 15.2$, $\times 12.7$ compared with HyperQ at when $\lambda = 0.8$ and the utilization is maximized in the first two benchmarks, and a factor $\times 6.5$, $\times 4.4$ when $\lambda = 0.6$ in the last two benchmarks. Below: Result of average fidelity. HALO remains competitive fidelity in Arithmetic benchmark and Mix benchmark, while is more sensitive to noise in QEC and $C^n(X)$ benchmark.

Benchmark	Algorithm	Space Utilization		Fidelity		PPB	
		Small	Medium	Small	Medium	Small	Medium
QEC	IBM Quantum	0.067	0.187	0.676	0.033	1	1
	HyperQ	0.111	0.353	0.666	0.046	1.71	1.85
	HALO (0.6)	0.618	0.669	0.340	0.007	15.79	9.58
Arithmetic	IBM Quantum	0.136	0.242	0.769	0.671	1	1
	HyperQ	0.292	0.309	0.714	0.571	1.6	1.33
	HALO (0.6)	0.817	0.810	0.647	0.547	14.92	7.54
$C^n(X)$	IBM Quantum	0.067	0.176	0.648	0.033	1	1
	HyperQ	0.128	0.279	0.666	0.046	1.85	1.6
	HALO (0.6)	0.739	0.923	0.340	0.007	12.08	5.69
Mix	IBM Quantum	0.133		0.614		1	
	HyperQ	0.330		0.487		2.29	
	HALO (0.6)	0.805 (↑2.44×)		0.327 (↓33%)		10.17 (↑4.44×)	

Table 4: Space utilization (utility), fidelity, and processes-per-batch (PPB) across benchmarks and scheduling configurations for HALO ($\lambda = 0.6$) vs. IBM Quantum vs. HyperQ. In the Mix benchmark, HALO achieves $2.44\times$ improvement in space utilization, a $4.44\times$ improvement in throughput while keeps the fidelity loss within 33% compared with HyperQ.

perQ’s fixed virtual-machine layout constraint and enabling explicit helper-qubit sharing, both of which are unavailable in HyperQ and jointly responsible for its severe fragmentation.

For fidelity, IBM Quantum and HyperQ maintain similar performance (49% and 46% on average), while HALO introduces a fidelity reduction of approximately 35% due to increased crosstalk and extra routing of qubit sharing (§3.5). However, this degradation is a tunable consequence of aggressive resource sharing and can be significantly reduced by lowering the data-occupancy ratio λ (discuss in § 4.6).

Take Benchmark II (the arithmetic benchmark, small circuits) as an example, where we populate the waiting queue with a mix of jobs that vary in both qubit usage. Under IBM Quantum, the system executes jobs strictly in FIFO order after

another, causing workloads with small space usage to dominate the hardware and resulting in low space utility (Table 4): IBM Quantum reaches a utility of 0.136, fidelity of 0.769, and only 1 process per batch. HyperQ mitigates this issue by enabling logical co-scheduling, increasing utility to 0.292 and processes per batch to 1.6, with fidelity 0.714.

In contrast, with $\lambda = 0.6$, HALO concurrently executes many more arithmetic jobs by reusing shared helper qubits and grouping tasks according to their space demands. On the same benchmark, HALO achieves utility 0.817 and 14.9 processes per batch, i.e., about a $9.3\times$ throughput improvement over HyperQ (and $15\times$ over IBM Quantum), while keeping fidelity at 0.647, only modestly below HyperQ (0.714). This illustrates how helper-qubit sharing delivers order-of-magnitude throughput gains at the cost of a relatively small fidelity reduction on practical workloads.

4.4 RQ3: Effectiveness of qubit sharing

To isolate the contribution of qubit resource sharing, we perform an ablation study comparing HALO to HALO(No Sharing), which disables helper-qubit reuse while retaining the same placement and scheduling strategy. As shown in Figure 6 and Table 5, HALO substantially increases processes per batch by allowing concurrently executing jobs to share helper qubits rather than reserving private helper qubit regions. Without sharing, a large fraction of physical qubits are forced to remain idle due to exclusive helper qubit reservation, particularly for workloads with high ancilla-to-data ratios such as the *Arithmetic* benchmark, where reversible logic synthesis introduces a heavy helper-qubit footprint [23, 48]. In

Benchmark	Configuration	Fidelity		PPB	
		Small	Medium	Small	Medium
QEC	HALO (0.6)	0.262	0.007	26.00	13.00
	HALO (No Sharing)	0.508	0.012	13.08	5.00
Arithmetic	HALO (0.8)	0.661	0.532	20.40	10.00
	HALO (No Sharing)	0.628	0.544	6.27	3.96
$C^n(X)$	HALO (0.6)	0.251	0.007	12.08	5.69
	HALO (No Sharing)	0.420	0.020	10.93	4.00
Mix	HALO (0.6)	0.327 (↑11%)		10.17 (↑1.52×)	
	HALO (No Sharing)	0.295		6.69	

Table 5: Comparison of fidelity and processes per batch (PPB) between HALO and HALO (No Sharing, but maximize space multiplexing). In the Mix benchmark, sharing helper qubits increase throughput by a factor $1.52\times$ while increase the fidelity by 11%.

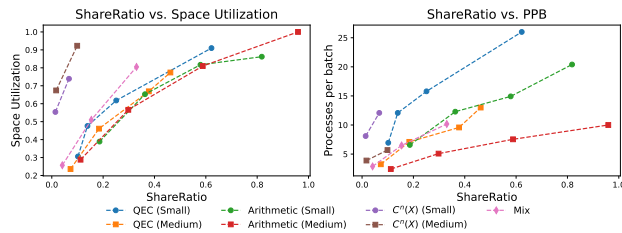


Figure 7: We plot the shareRatio with space utilization and PPB for all our benchmark. The result consistently show that the more qubit we allow HALO to share, the larger the throughput and the space utilization.

this setting, HALO(No Sharing) achieves only 6.27 and 3.96 processes per batch (small/medium), whereas HALO reaches 20.40 and 10.00, corresponding to a $3.25\times$ and $2.53\times$ improvement in throughput, respectively. This translates to a 69–76% reduction in average waiting time for users under sustained load. In the Mix benchmark, HALO(0.6) increase throughput by a factor of $1.52\times$ while increase the fidelity by 11%.

Figure 7 indicates that the increase in space utility and throughput is a direct result of sharing helper qubits. The utility and PPB increase consistently with ShareRatio across all benchmarks. In the most aggressive case, Share ratio approaches 1, which indicates that almost all helper qubits are used by more than 2 different processes. The results match our expectation illustrated in Figure 1(§1). In conclusion, we prove the value of sharing helper qubits: *The more we share helper qubits, the larger throughput gain we will have.*

4.5 RQ4: Effectiveness of shot-aware batch scheduling

To study the effectiveness of our Shot-aware batch scheduling algorithm, we run HALO scheduling on a process queue randomly selected from all benchmark circuits. All process has a randomly generated shots value that ranges between 500

	Space time utility η		Fidelity		
	Aware	Unaware	Improve	Aware	Unaware
HALO(0.2)	0.235	0.082	$\times 2.87$	0.493	0.483
HALO(0.4)	0.373	0.083	$\times 4.49$	0.427	0.429
HALO(0.6)	0.460	0.114	$\times 4.04$	0.380	0.415

Table 6: Space–time utilization and fidelity on the Mix benchmark for shot-aware and shot-unaware scheduling.

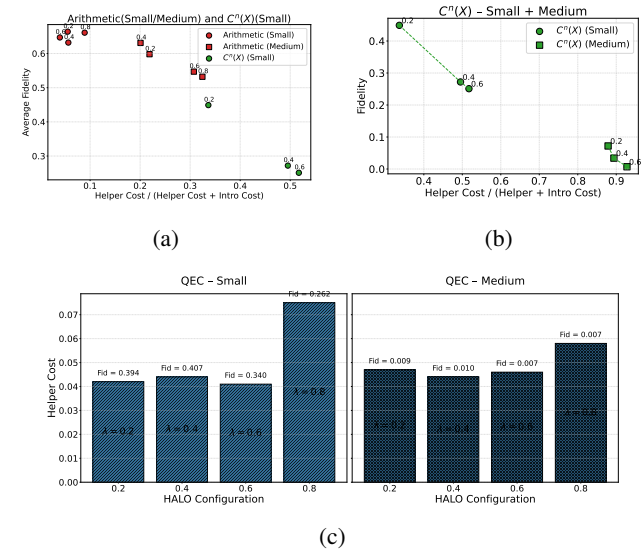


Figure 8: We study the relation between fidelity with $HRCost(L, G)$ and ratio of helper qubit routing cost in HALO: $\frac{HRCost(L, G)}{Intro(G, L) + HRCost(L, G)}$. In (a),(b), we observe a strong correlation between the ratio with the final fidelity. In QEC benchmark, the ratio is always 1, and the fidelity degradation can be explained by increase of $HRCost(L, G)$

to 8000. We run the same experiments for HALO algorithm with both 1. *Shot-unaware* batch scheduling, where the next batch is taken from the queue according to the FIFO order. 2. *Shot-aware* batch scheduling (§3.4). We tune the *data occupancy ratio* λ from 0.2 to 0.6 and repeat the same experiment. The results in Table 6 shows our Shot-aware batch scheduling consistently improve the space time utility η by a factor of $\times 2.87, \times 4.49, \times 4.04$. Moreover, the fidelity of HALO with shot-unaware batch scheduling is close to the fidelity with shot-aware batch scheduling. We conclude that shot-aware scheduling does not harm the fidelity.

4.6 RQ5: Throughput-fidelity trade-off and explanation

We observe the tradeoff between the averaged fidelity and the throughput. When aggressive qubit sharing is allowed, the fidelity of all benchmarks degrade. Especially for the QEC benchmark and $C^n(X)$ benchmark.

To understand the difference between the fidelity degra-

dation level in different benchmarks, we analyze all the cost functions of the results (§3.5). We can explain the difference well by the ratio of routing cost of helper qubit, calculated as $\frac{\text{HRCost}(L,G)}{\text{Intro}(G,L) + \text{HRCost}(L,G)}$ (§3.5), which quantifies how much of the total routing overhead comes specifically from accessing helper qubits. A higher ratio indicates that a larger fraction of noise is introduced by helper-qubit routing and reuse. This ratio is highly sensitive to the λ , as λ increases, more physical qubits are allocated as data qubits, forcing helper qubits to be shared across more processes. This increases both the distance and frequency of data-helper interactions, and thus the helper-routing cost. In the QEC benchmark, where each data qubit depends on many helper qubits, the ratio is always 1, meaning all additional routing noise is caused by accessing helper qubits—this explains why HALO performs worst on QEC workloads.

In contrast, for Arithmetic and $C^n(X)$ circuits, the fidelity decreases roughly linearly with this ratio (Figure 8). The medium-scale $C^n(X)$ benchmark represents the worst non-QEC case: almost all routing overhead comes from helper access, resulting in fidelity below 10%. Conversely, in the Arithmetic benchmark, less than half of the routing cost originates from helper-qubit interaction, allowing HALO to maintain substantially higher fidelity even as λ increases.

For QEC circuits which are heavily ancilla-intensive and $\text{Intro}(G,L)$ is always 0, we study the fidelity degradation with $\text{HRCost}(L,G)$. Bar plot (c) in Figure 8 indicates the degradation comes from the increase of $\text{HRCost}(L,G)$ cost itself. In summary, helper qubit routing and sharing have a more severe effect on circuit fidelity than intro circuit data qubit routing in HALO. Despite the tradeoff, we expect that HALO’s performance will keep increasing with the improvement of quantum hardware towards fault-tolerance in the next few years [5, 18].

5 Related Work

Quantum virtualization and multi-tenant execution. Several recent systems explore ways to allow multiple quantum programs to coexist on a single device. HyperQ [47] introduces virtual quantum machines (qVMs) to multiplex circuits on cloud hardware and demonstrates that concurrency can reduce user-perceived latency. QOS [19] similarly provides abstractions for job submission, device sharing, and execution monitoring. While these systems significantly advance the software stack for cloud quantum computing, they do not exploit opportunities for fine-grained physical resource sharing. In contrast, HALO enables both spatial and temporal sharing at the hardware level by reusing helper qubits and incorporating shot-adaptive scheduling.

Resource sharing in classical operating systems. Resource sharing is a foundational capability of classical op-

erating systems, which multiplex CPU, memory, and I/O using long-established mechanisms such as time-sharing, virtual memory [21], and modern isolation tools such as cgroups [32]. User-level threading and scheduler-activation techniques further illustrate how CPU and execution contexts can be multiplexed efficiently [8]. These abstractions provide efficiency, isolation, and fairness for multi-process workloads. For emerging quantum computers, the underlying resources are qubits that are fragile, non-clonable, and coherence-limited. HALO introduces new system abstractions and designs to re-establish practical resource sharing in this setting.

Qubit layout synthesis and routing. Quantum layout synthesis maps logical qubits and operations onto hardware with constrained connectivity, requiring efficient placement and routing to minimize SWAP overhead and mitigate noise. A rich body of work has optimized initial mapping and routing heuristics for single-circuit compilation [30, 36, 52]. Tan and Cong [46] demonstrated significant optimality gaps in state-of-the-art mapping tools, with generated circuits frequently being 5–45× deeper than optimal. Their findings underscore the importance of topology-aware compilation for maintaining fidelity in today’s hardware. Prior work assumes a single monolithic circuit and focuses on reducing qubit count through ancilla reuse within a circuit’s computation [40]. In contrast, HALO introduces a multi-process placement and routing strategy that allows helper qubits to be safely reassigned across concurrently executing circuits. This design introduces new constraints not captured in existing formulations, including inter-process crosstalk avoidance and prevention of unintended entanglement across workloads. To the best of our knowledge, HALO is the first system to enable inter-process helper-qubit reuse while preserving correctness and isolation guarantees.

6 Conclusion

We propose HALO, the first fine-grained resource sharing quantum operating system. HALO significantly increases the throughput compared to the state-of-the-art approaches in helper qubit-intensive applications by 4.44×, while maintains a competitive fidelity within 33% of loss (Table 4). Our analysis of experiments data prove that the fidelity degradation primarily arises from the additional routing, reset operations, and helper-qubit reuse required at higher occupancy levels. Thus, HALO provides a fidelity throughput tradeoff and is adaptable for different users’ requirements.

Artifact

We release our artifact and data in the anonymous repository: <https://anonymous.4open.science/r/HALO-C814/>.

References

- [1] Fair-share scheduler. <https://quantum.cloud.ibm.com/docs/guides/fair-share-scheduler>. IBM Quantum Docs, accessed Oct. 23, 2025.
- [2] When will my quantum task run? <https://docs.aws.amazon.com/braket/latest/developerguide/braket-task-when.html>. Amazon Braket Docs, accessed Oct. 23, 2025.
- [3] Why does job appear to be stuck in queue on ibmq backend? <https://quantumcomputing.stackexchange.com/questions/13878/why-does-job-appear-to-be-stuck-in-queue-on-ibmq-backend>. StackExchange, accessed Dec 3, 2025.
- [4] Working with reservations. <https://docs.aws.amazon.com/braket/latest/developerguide/braket-reservations.html>. Amazon Braket Docs, accessed Oct. 23, 2025.
- [5] Suppressing quantum errors by scaling a surface code logical qubit. *Nature*, 614(7949):676–681, 2023.
- [6] Muhammad AbuGhanem. Ibm quantum computers: evolution, performance, and future directions. *arXiv preprint arXiv:2410.00916*, 2024.
- [7] Janet Anders, Daniel KL Oi, Elham Kashefi, Dan E Browne, and Erika Andersson. Ancilla-driven universal quantum computation. *Physical Review A—Atomic, Molecular, and Optical Physics*, 82(2):020301, 2010.
- [8] Thomas E. Anderson, Brian N. Bershad, Edward D. Lazowska, and Henry M. Levy. Scheduler activations: Effective kernel support for the user-level management of parallelism. In *Proceedings of the 13th ACM Symposium on Operating Systems Principles (SOSP)*, pages 95–109, 1991.
- [9] Frank Arute, Kunal Arya, Ryan Babbush, Dave Bacon, Joseph C Bardin, Rami Barends, Rupak Biswas, Sergio Boixo, Fernando GSL Brandao, David A Buell, et al. Quantum supremacy using a programmable superconducting processor. *Nature*, 574(7779):505–510, 2019.
- [10] Sergey Bravyi and Jeongwan Haah. Magic-state distillation with low overhead. *Physical Review A—Atomic, Molecular, and Optical Physics*, 86(5):052329, 2012.
- [11] Katherine L Brown, Suvabrata De, Vivien M Kendon, and William J Munro. Ancilla-based quantum simulation. *New Journal of Physics*, 13(9):095007, 2011.
- [12] Colin D Bruzewicz, John Chiaverini, Robert McConnell, and Jeremy M Sage. Trapped-ion quantum computing: Progress and challenges. *Applied physics reviews*, 6(2), 2019.
- [13] Mosharaf Chowdhury and Ion Stoica. Efficient coflow scheduling without prior knowledge. *ACM SIGCOMM Computer Communication Review*, 45(4):393–406, 2015.
- [14] John Clarke and Frank K Wilhelm. Superconducting quantum bits. *Nature*, 453(7198):1031–1042, 2008.
- [15] Andrew J Daley, Immanuel Bloch, Christian Kokail, Stuart Flannigan, Natalie Pearson, Matthias Troyer, and Peter Zoller. Practical quantum advantage in quantum simulation. *Nature*, 607(7920):667–676, 2022.
- [16] Peter J Denning. Virtual memory. *ACM Computing Surveys (CSUR)*, 2(3):153–189, 1970.
- [17] Mohammad Javad Dousti, Alireza Shafaei, and Massoud Pedram. Squash: a scalable quantum mapper considering ancilla sharing. In *Proceedings of the 24th Edition of the Great Lakes Symposium on VLSI, GLSVLSI '14*, page 117–122, New York, NY, USA, 2014. Association for Computing Machinery.
- [18] Simon J Evered, Dolev Bluvstein, Marcin Kalinowski, Sepehr Ebadi, Tom Manovitz, Hengyun Zhou, Sophie H Li, Alexandra A Geim, Tout T Wang, Nishad Maskara, et al. High-fidelity parallel entangling gates on a neutral-atom quantum computer. *Nature*, 622(7982):268–272, 2023.
- [19] Emmanouil Giortamis, Francisco Romão, Nathaniel Tornow, and Pramod Bhatotia. Qos: a quantum operating system. *arXiv preprint arXiv:2406.19120*, 2024.
- [20] Nicolas Gisin and Helle Bechmann-Pasquinucci. Bell inequality, bell states and maximally entangled states for n qubits. *Physics Letters A*, 246(1-2):1–6, 1998.
- [21] Robert P. Goldberg. Survey of virtual machine research. *Computer*, 7(6):34–45, 1974.
- [22] Lov K. Grover. A fast quantum mechanical algorithm for database search, 1996.
- [23] Thomas Haener, Mathias Soeken, Martin Roetteler, and Krysta M Svore. Quantum circuits for floating-point arithmetic. In *International Conference on Reversible Computation*, pages 162–174. Springer, 2018.
- [24] Ellen L. Hahne. Round-robin scheduling for max-min fairness in data networks. *IEEE Journal on Selected Areas in communications*, 9(7):1024–1039, 2002.
- [25] Tianyi Hao, Zichang He, Ruslan Shaydulin, Jeffrey Larson, and Marco Pistoia. End-to-end protocol for high-quality quantum approximate optimization algorithm parameters with few shots. *Physical Review Research*, 7(3), August 2025.

[26] Ryszard Horodecki, Paweł Horodecki, Michał Horodecki, and Karol Horodecki. Quantum entanglement. *Reviews of modern physics*, 81(2):865–942, 2009.

[27] Keli Huang and Jens Palsberg. Compiling conditional quantum gates without using helper qubits. *Proc. ACM Program. Lang.*, 8(PLDI), June 2024.

[28] HV Jayashree, Himanshu Thapliyal, Hamid R Arabnia, and Vinod Kumar Agrawal. Ancilla-input and garbage-output optimized design of a reversible quantum integer multiplier. *The Journal of Supercomputing*, 72(4):1477–1493, 2016.

[29] Ang Li, Samuel Stein, Sriram Krishnamoorthy, and James Ang. Qasmbench: A low-level quantum benchmark suite for nisq evaluation and simulation. *ACM Transactions on Quantum Computing*, 4(2):1–26, 2023.

[30] Gushu Li, Yu Zhou, Yuwei Ding, Yuan Xie, and Hong Cheng. Tackling the qubit mapping problem for nisq-era quantum devices. In *ASPLOS*, 2019.

[31] Daniel Litinski. A game of surface codes: Large-scale quantum computing with lattice surgery. *Quantum*, 3:128, March 2019.

[32] Paul Menage. Cgroups. Technical report, Google, 2007.

[33] D Michael Miller, Robert Wille, and Zahra Sasanian. Elementary quantum gate realizations for multiple-control toffoli gates. In *2011 41st IEEE international symposium on multiple-valued logic*, pages 288–293. IEEE, 2011.

[34] Abtin Molavi, Amanda Xu, Martin Diges, Lauren Pick, Swamit Tannu, and Aws Albarghouthi. Qubit mapping and routing via maxsat. In *Proceedings of the 55th Annual IEEE/ACM International Symposium on Microarchitecture*, MICRO ’22, page 1078–1091. IEEE Press, 2023.

[35] Mario Motta, Chong Sun, Adrian TK Tan, Matthew J O’Rourke, Erika Ye, Austin J Minnich, Fernando GSL Brandao, and Garnet Kin-Lic Chan. Determining eigenstates and thermal states on a quantum computer using quantum imaginary time evolution. *Nature Physics*, 16(2):205–210, 2020.

[36] Prakash Murali, Nathan Baker, Ali Javadi-Abhari, Alexander McCaskey, Travis Humble, and Frederic Chong. Noise-adaptive compiler mappings for noisy intermediate-scale quantum computers. In *ASPLOS*, 2019.

[37] Michael A Nielsen and Isaac L Chuang. *Quantum computation and quantum information*. Cambridge university press, 2010.

[38] Rasmus V Rasmussen and Michael A Trick. Round robin scheduling—a survey. *European Journal of Operational Research*, 188(3):617–636, 2008.

[39] Diego Riste, Stefano Poletto, M-Z Huang, Alessandro Bruno, Visa Vesterinen, O-P Saira, and Leonardo Di-Carlo. Detecting bit-flip errors in a logical qubit using stabilizer measurements. *Nature communications*, 6(1):6983, 2015.

[40] Ritvik Sharma and Sara Achour. Optimizing ancilla-based quantum circuits with spare. *Proceedings of the ACM on Programming Languages*, 9(PLDI):176–200, 2025.

[41] Peter W Shor. Fault-tolerant quantum computation. In *Proceedings of 37th conference on foundations of computer science*, pages 56–65. IEEE, 1996.

[42] P.W. Shor. Algorithms for quantum computation: discrete logarithms and factoring. In *Proceedings 35th Annual Symposium on Foundations of Computer Science*, pages 124–134, 1994.

[43] Madhavapeddi Shreedhar and George Varghese. Efficient fair queuing using deficit round-robin. *IEEE/ACM Transactions on networking*, 4(3):375–385, 1996.

[44] Jasmine Sinanan-Singh, Gabriel L Mintzer, Isaac L Chuang, and Yuan Liu. Single-shot quantum signal processing interferometry. *Quantum*, 8:1427, 2024.

[45] Matthias Steffen, David P DiVincenzo, Jerry M Chow, Thomas N Theis, and Mark B Ketchen. Quantum computing: An ibm perspective. *IBM Journal of Research and Development*, 55(5):13–1, 2011.

[46] Bochen Tan and Jason Cong. Optimal layout synthesis for quantum computing. In *Proceedings of the 39th International Conference on Computer-Aided Design*, pages 1–9, 2020.

[47] Runzhou Tao, Hongzheng Zhu, Jason Nieh, Jianan Yao, and Ronghui Gu. Quantum virtual machines. USENIX, 2025.

[48] Michael Kirkedal Thomsen, Robert Glück, and Holger Bock Axelsen. Reversible arithmetic logic unit for quantum arithmetic. *Journal of Physics A: Mathematical and Theoretical*, 43(38):382002, 2010.

[49] Peter JM Van Laarhoven and Emile HL Aarts. Simulated annealing. In *Simulated annealing: Theory and applications*, pages 7–15. Springer, 1987.

[50] Will Zeng, Blake Johnson, Robert Smith, Nick Rubin, Matt Reagor, Colm Ryan, and Chad Rigetti. First quantum computers need smart software. *Nature*, 549(7671):149–151, 2017.

- [51] Peng Zhao, Kehuan Linghu, Zhiyuan Li, Peng Xu, Ruixia Wang, Guangming Xue, Yirong Jin, and Haifeng Yu. Quantum crosstalk analysis for simultaneous gate operations on superconducting qubits. *PRX quantum*, 3(2):020301, 2022.
- [52] Yufei Zhou, Gushu Li, Yuwei Ding, Hong Cheng, and Yuan Xie. Quartz: Efficient synthesis of quantum circuits. In *ASPDAC*, 2020.
- [53] Ben Zindorf and Sougato Bose. Efficient implementation of multi-controlled quantum gates, 2025.